

# The Focusing Optics X-ray Solar Imager: FOXSI

Säm Krucker<sup>a</sup>, Steven Christe<sup>a</sup>, Lindsay Glesener<sup>a,b</sup>, Steve McBride<sup>a</sup>, Paul Turin<sup>a</sup>, David Glaser<sup>a</sup>, Pascal Saint-Hilaire<sup>a</sup>, Gregory Delory<sup>a</sup>, Robert P. Lin<sup>a,b</sup>, Brian Ramsey<sup>b</sup>, Mikhail Gubarev<sup>b</sup>, Shin-nosuke Ishikawa<sup>d,e</sup>, Tadayuki Takahashi<sup>d,e</sup>, Hiroyasu Tajima<sup>f</sup>, Satoshi Masuda<sup>g</sup>

<sup>a</sup>Space Sciences Lab, U.C. Berkeley, 7 Gauss Way, Berkeley, CA 94720-7450

<sup>b</sup>Physics Department, U.C. Berkeley, Berkeley, CA 94720

<sup>c</sup>MSFC/NASA, Huntsville, AL 35812

<sup>d</sup>Institute of Space and Astronautical Science, Sagami-hara, Kanagawa 229-8510, Japan

<sup>e</sup>Department of Physics, University of Tokyo, Hongou, Bunkyo-ku, Tokyo, 113-0033, Japan

<sup>f</sup>Stanford Linear Accelerator Center, Stanford, CA 94309-4349

<sup>g</sup>Solar-Terrestrial Environment Laboratory, Nagoya University, Furo-cho, Chikusa-ku, Nagoya 464-8601, Japan

## ABSTRACT

The Focusing Optics X-ray Solar Imager (*FOXSI*) is a sounding rocket payload funded under the NASA Low Cost Access to Space program to test hard X-ray focusing optics and position-sensitive solid state detectors for solar observations. Today's leading solar hard X-ray instrument, the Reuven Ramaty High Energy Solar Spectroscopic Imager (*RHESSI*) provides excellent spatial (2 arcseconds) and spectral (1 keV) resolution. Yet, due to its use of indirect imaging, the derived images have a low dynamic range (<10) and sensitivity. These limitations make it difficult to study faint x-ray sources in the solar corona which are crucial for understanding the solar flare acceleration process. Grazing-incidence x-ray focusing optics combined with position sensitive solid state detectors can overcome both of these limitations enabling the next breakthrough in understanding particle acceleration in solar flares. The *FOXSI* project is led by the Space Science Laboratory at the University of California. The NASA Marshall Space Flight Center, with experience from the *HERO* balloon project, is responsible for the grazing-incidence optics, while the Astro H team (JAXA/ISAS) will provide double-sided silicon strip detectors. *FOXSI* will be a pathfinder for the next generation of solar hard X-ray spectroscopic imagers. Such observatories will be able to image the nonthermal electrons within the solar flare acceleration region, trace their paths through the corona, and provide essential quantitative measurements such as energy spectra, density, and energy content in accelerated electrons.

**Keywords:** sounding rocket payload, solar physics, nanoflares, silicon strip detectors, grazing-incidence optics, high-energy x-ray optics, electroform-nickel replication

## 1. INTRODUCTION

Hard X-ray (HXR) observations are a powerful diagnostic tool providing quantitative measurements of accelerated nonthermal electron beams, in particular, in solar flares. Energetic electrons traveling in a plasma radiate HXR emission through the well known process of bremsstrahlung. It is thought that electrons are accelerated somewhere in the solar atmosphere (the corona) and travel along magnetic field lines. Since bremsstrahlung emission depends on the density of the ambient medium, solar HXR emission is largest when electrons are stopped by the solar "surface". Electron beams entering the chromosphere lose energy quickly through collisions, producing relatively intense HXR emission at the footpoints of magnetic field lines. Energetic electrons moving in the relatively tenuous corona suffer only a few collisions, losing little energy and producing only faint HXR emission. Present-day instrumentation does not have the sensitivity to see faint HXR emission from electrons

---

Further author information: (Send correspondence to S. Krucker)

S. Krucker: E-mail: krucker@ssl.berkeley.edu, Telephone: 1 510 643 3101

S. Christe: E-mail: schriste@ssl.berkeley.edu, Telephone: 1 510 643 5648

traveling through the corona, nor the dynamic range to see such faint emission in the presence of bright HXR footpoint emission in the chromosphere. Existing observations therefore show us only where energetic electrons are stopped but not where they are accelerated, nor along what path they escape from the acceleration site. Thus, to make the next breakthrough in understanding the acceleration process requires HXR imaging with much higher sensitivity and dynamic range. HXR focusing optics can provide both.

The most sensitive solar HXR observations so far are provided by the Reuven Ramaty High Spectroscopic Imager (*RHESSI*).<sup>1</sup> These measurements are obtained with a non-focusing, rotation modulation collimator (RMC) imaging technique.<sup>2</sup> RMCs and other types of non-focusing imaging, however, have intrinsically limited dynamic range and sensitivity. Through focusing both of these limitations can be overcome. Recent developments in x-ray focusing optics have extended the range of focusable energies well into the HXR range. New focusing x-ray optics telescopes have been developed at the Marshall Space Flight Center (MSFC) and successfully flown on balloons to observe astrophysical objects.<sup>3</sup> Coupled with new position sensitive solid state detectors which can do spectroscopy on individual pixels, new HXR observations with unprecedented sensitivity and dynamic range are now possible. We present a new instrument which applies these technologies to solar observations via a sounding-rocket payload.

Called *FOXSI*, short for the Focusing Optics X-ray Solar Imager, this instrument will feature an array of grazing-incidence mirror modules focusing to a corresponding array of silicon focal plane detectors. *FOXSI* is expected to be  $\sim 50$  times more sensitive than *RHESSI* at 10 keV with up to 100 times larger dynamic range. The high sensitivity of *FOXSI* will for the first time allow a search for HXR counterparts of flares seen in the quiet corona.<sup>4-6</sup> The existence of such emission would suggest that nanoflares are an important part of the coronal heating problem.

## 2. OVERVIEW

*FOXSI* is a sounding rocket program funded by the NASA Low Cost Access to Space (LCAS) program. Led by the Space Sciences Laboratory (SSL) at U.C. Berkeley, the *FOXSI* program also involves the NASA Marshall Space Flight Center (MSFC), and the Astro-H team. *FOXSI* will apply new HXR focusing optics developed for astrophysical observations to solar observations. A major goal for the *FOXSI* program is to push these developing technologies for to the unique requirements of solar observations; the most important of which are high spatial resolution, large dynamic range and fast counting rates.

The tasks of the *FOXSI* program are neatly divided among the various institutions involved. The optics are being developed and manufactured at the MSFC under the direction of Dr. Brian Ramsey. The *FOXSI* detectors are being developed by ISAS/JAXA as part of the Astro-H mission (formerly NeXT) led by Prof. Tadayuki Takahashi.<sup>7</sup> They consist of silicon Double-Sided Strip Detectors (DSSD) which are fabricated by Hamamatsu and read out by Application Specific Integrated Circuits (ASICs) designed and built by Gamma Medica-Ideas (Norway). SSL is leading this effort and is designing and constructing the physical payload, including the detector read-out electronics.

The *FOXSI* instrument is composed of 7 grazing-incidence telescope modules, each with 7 nested shells. Due to constraints imposed by the rocket payload size, the *FOXSI* focal length is 2 m. This (relatively) short focal length limits the highest energy at which significant area can be achieved to about 20 keV, which matches well with the efficiency of the silicon detectors. Noise in the detectors may limit the lowest detectable energies to  $\sim 5$  keV. The total effective area is expected to be  $\sim 180$  cm<sup>2</sup> from  $\sim 5$  to 10 keV, falling to  $\sim 14$  cm<sup>2</sup> at 15 keV (see Figure 2). *FOXSI* will have a field of view of approximately  $960 \times 960$  arcseconds (HPW) which covers approximately a quarter of the solar disk. The current typical angular resolution (FWHM) for modules containing multiple nested shells is  $\sim 12$  arcseconds, which is limited by misalignment between the component shells. A new process is expected to improve the alignment process (see Section 4) so that the resolution of a module will be close to that of individual shells. A  $128 \times 128$  strip,  $500 \mu\text{m}$  thick double-sided silicon strip detector with  $75 \mu\text{m}$  strip pitch will cover the detector plane. The expected energy resolution of *FOXSI* is around 1 keV. The combination of small detector size and large effective area leads us to expect that the sensitivity of *FOXSI* will be  $\sim 50$  times better than *RHESSI*. Table 1 summarizes the properties of the *FOXSI* instrument.

Table 1. *FOXSI* Overview.

<b>Optics Characteristics:</b>	
Angular Resolution (FWHM)	7 arcseconds (single shell), 12 arcseconds (module)
Number of modules	7
Number of shells per module	7
Focal length	2 m (Wolter I)
<b>Detector Characteristics:</b>	
Type	Double-sided Silicon Strip Detectors
Thickness	500 $\mu\text{m}$
Energy Resolution	$\sim 1$ keV (FWHM)
Low Energy Threshold	$\sim 5$ keV
Detector Pitch	75 $\mu\text{m}$
Dimensions	128 $\times$ 128 strips (9.6 $\times$ 9.6 mm <sup>2</sup> )
<b>Telescope Characteristics</b>	
Energy range	$\sim 5$ to 15 keV (200 $\mu\text{m}$ Be entrance window)
Field of View	960 $\times$ 960 arcseconds
Effective area	$\sim 180$ cm <sup>2</sup> (8 keV), $\sim 14$ cm <sup>2</sup> at 15 keV
Sensitivity ( $\sim 8$ keV)	$\sim 0.004$ cm <sup>-2</sup> s <sup>-1</sup> keV <sup>-1</sup> ( $\sim 50$ times <i>RHESSI</i> )
Dynamic Range	100 for source separation $> 30$ arcseconds
<b>Id. Mission Characteristics</b>	
Observation time	$\sim 360$ s

### 3. PAYLOAD DESIGN

The FOXSI payload design is heavily influenced by the existing HERO design.<sup>3</sup> The payload will be oriented “backwards” in the rocket casing in order to minimize rocket separation events. Shedding of the last rocket engine will reveal a hinged door in front of the FOXSI optics. Pointing control systems will then reorient the payload sunward. The NASA-provided Solar Pointing Attitude Rocket Control System (SPARCS) system will provide high-stability programmable solar pointing. Located behind the detector end of the payload are various rocket control systems and the rocket nose cone containing a recovery parachute. Since recovery of the payload is required the launch will take place at the NASA White Sands Test Facility in New Mexico.

There are two basic mechanical requirements to the telescope assembly: it must properly position the seven telescope modules with their respective detectors and it must provide an optimal thermal environment for the telescope components. Structurally, the telescope modules mount to a circular aluminum plate, approximately 17 inches in diameter (See Figure 1), which in turn is riveted to a precision rolled aluminum tube that spans the entire 2 m focal length (See Figure 2). The opposite end of the tube is riveted to a ring, to which a detector plate—containing the seven detectors—is fastened. The rigidity of the tube and the two riveted ends provides the axial alignment of the telescope modules with the detectors. This tube assembly mounts to the rocket only from the optical end, via a larger aluminum plate that is fastened directly to the rocket skin (See Figure 2). The detector end of the tube is cantilevered so that it will not be structurally indeterminate, and also to not have any conductive thermal contact with the rocket skin.

Thermally, the optics require a stable temperature of  $25 \pm 2^\circ$  Celsius, the detectors must be kept below  $-20^\circ$  Celsius, and the detector electronics need a temperature between zero and  $50^\circ$  Celsius. During flight, the rocket skin will heat up to  $\sim 150^\circ$  Celsius. The optics temperature will be controlled by a xxx, but the detectors will be cooled passively. The detectors are mounted in the much larger thermal mass of the mounting plate. Prior to launch, the temperature of this plate will be actively cooled to  $-30^\circ$  Celsius with LN2, which will be piped into a sealed channel inside the plate from a dewar external to the rocket. The vaporized nitrogen will then pass into the cavity where each detector is held in order to prevent the build up of water moisture while the rocket is in its pre-launch preparations.

The active and passive cooling of the optics and detector assemblies is aided by placement of insulating materials. Each telescope module is completely surrounded by a blanket of multi-layered insulation (MLI),

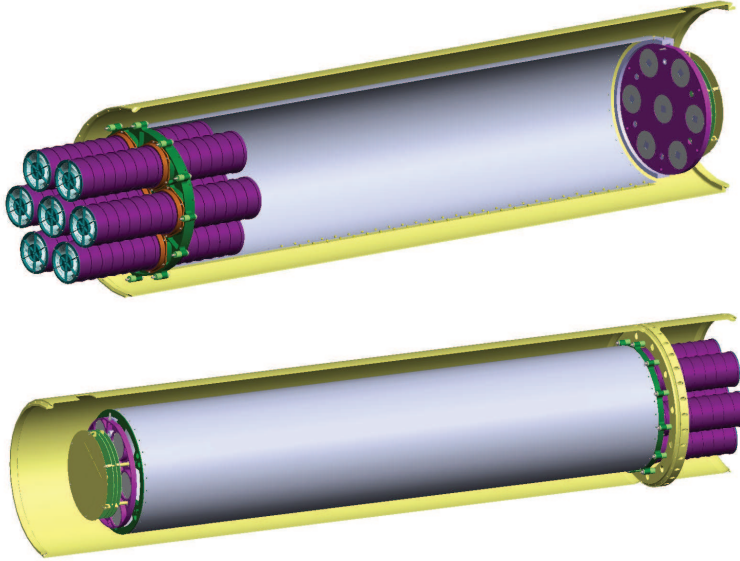


Figure 1. Diagram of the optical arrangement of the payload inside a 22 in rocket skin. *Top:* The basic structure of the payload consists of a 2-m-long rolled aluminum tube (shown in cutaway) that hold the array of 7 optics and 7 detectors, mounted on an aluminum ring one end, and an aluminum plate holding the 7 detectors at the opposite end. The payload will be oriented “backwards” within the rocket as the detector end is located at the front of the rocket. Separation of the rocket engine will allow the optics to be revealed. *Bottom:* The aluminum tube is made rigid at its ends by the optics mounting plate and the focal plane mounting ring (both shown in green) and this structure is cantilevered inside the rocket skin by a larger mounting ring (yellow) that is fastened to the rocket skin. The detector electronics (right) are mounted on aluminum standoffs forward of the detectors.

which blocks most of the radiative heat transfer and the optics mounting plate is conductively isolated from the mounting ring by fiberglass standoffs. The detector plate is surrounded by a one-half inch layer of *Basotect* foam<sup>8</sup> that is in turn covered with aluminized mylar. The detector plate is also thermally isolated from its mounting ring by a set of fiberglass standoffs. The detector electronics, which generate  $\sim 30$  W of heat, are mounted on aluminum standoffs that fasten—and conduct heat—to the focal plane mounting ring, while being insulated with foam from the detector plate. Finally, the entire telescope tube assembly is wrapped in a blanket of MLI that cuts down radiative heat transfer from the rocket skin. Thermal modeling predicts that, during the 6 min flight, the temperature of the detector plate will rise less than  $2^\circ$  Celsius from its starting temperature of  $-30^\circ$  Celsius.

#### 4. OPTICS

Past grazing-incidence X-ray telescopes, such as the Chandra X-ray Observatory, employ large mirrors which are each individually polished to a high precision finish. At high energies, grazing incidence reflectivities are small which implies that many mirrors are needed to provide significant area. Producing many such individually polished mirrors is prohibitively expensive. A new process, electroform nickel replication, uses a single highly polished form (mandrel) which is electro-coated to produce individual mirrors. Such mirrors do not need to be polished since they retain the finish and shape of the polished mandrel. Additionally, a mandrel can produce many telescope shells that can be nested to provide significant area in the HXR range. This process has been implemented successfully for HXR astronomy in the *HERO* balloon program<sup>3</sup> at the MSFC.

The reflectivity of nickel at 10 keV falls off quickly at graze angles above 0.5 degrees. This sets the maximum shell radius to  $\sim 5$  cm for the energies of interest and a focal length of 2 m (see Table 2). Within a standard 22 in. rocket diameter, 7 modules with this radius can be accommodated (see Figure 1).

The angular resolution of an individual mirror shell depends upon the figure of the shell and is independent of the focal length or radius of the mirror shells. For astrophysical applications, the half-power diameter (HPD) is the accepted metric for the optic resolution. For solar observations, the full width at half maximum (FWHM)

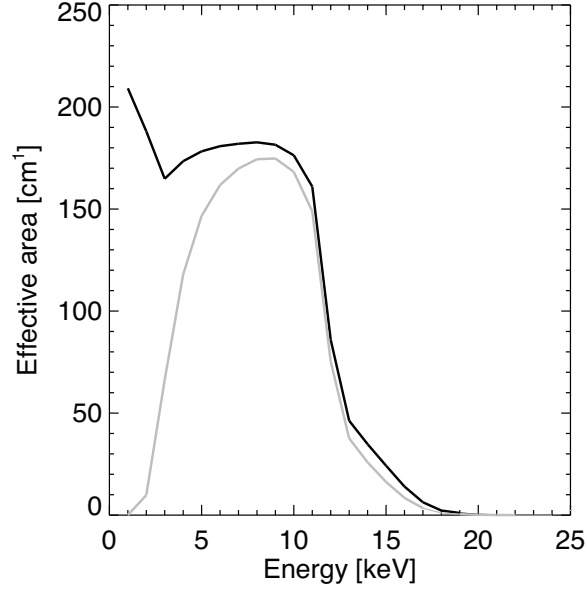


Figure 2. The total *FOXSI* effective area as a function of energy. The black curve represents the area provided by the optics. The gray curve shows the effective area after including detector efficiency and absorption by thermal blanketing.

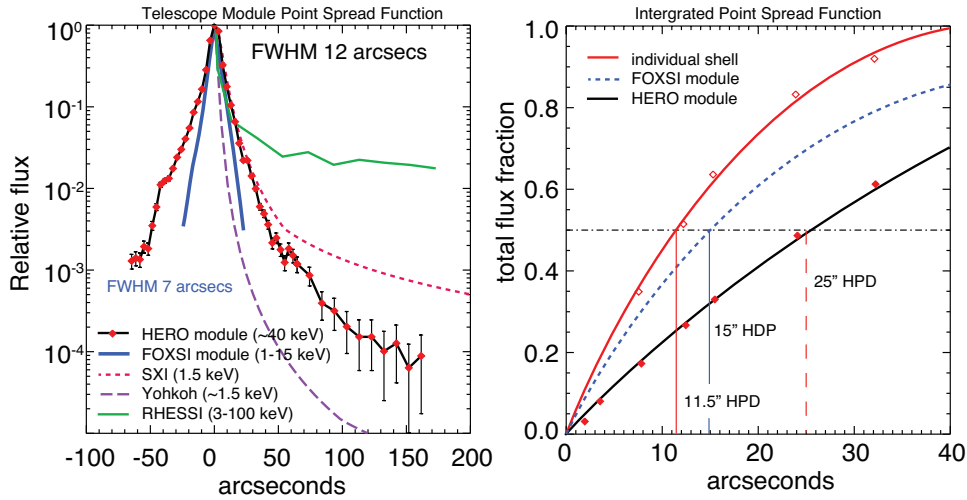


Figure 3. *Left*: The measured point spread function for a *HERO* telescope module made up of 15 nested shells compared to other similar X-ray instruments. *RHESSI* is the only non-focusing imager and the only solar instrument in HXR range. The *HERO* PSF falls off rapidly; 2 orders of magnitude within  $\sim 30$  arcseconds. The expected inner point spread function for a *FOXSI* module is also shown with the expected FWHM of 7 arcseconds. *Right*: The integrated point spread function of the same *HERO* module as compared to an existing single shell. A *FOXSI* module is also shown.

Table 2. Detailed Optics characteristics.

Focal length	2 m
Form	Wolter I
Number of shells	7
Outer shell radius	51.51 mm
Inner shell radius	37.99 mm
Shell length	60 cm
Shell thickness	250 $\mu\text{m}$
Coating	30 nm Iridium

is a more appropriate measure. Single shells with a FWHM down to  $\sim 7$  arcseconds have already been produced. The spatial resolution of a telescope module is currently limited to  $\sim 12$  arcseconds by the nesting assembly process (e.g. HERO, Figure 3); individual shells are not perfectly aligned and distortions are imparted by the mounting system. A new nesting process has been developed whereby the shells are carefully monitored as they are being set and mounting clips are used to minimize deformation by the contact points.<sup>9</sup> This new process will be used on the *FOXSI* modules and is expected to improve the module resolution to the resolution of individual shells ( $\sim 7$  arcseconds).

The point spread function (PSF) of a *HERO* telescope module is compared to other X-ray imagers in Figure 3. As compared to astronomical HXR observations, which rarely contain more than one source in the field of view, solar flare observations very often show many sources close to one another. The shape of the PSF is therefore very important since a single source may contribute a significant “background” for nearby sources. The PSF sets the dynamic range of the image. This problem is well illustrated by *RHESSI* which uses indirect imaging. The dynamic range is low ( $<30$ , typically  $\sim 5$ ), since each detector can see the entire field of view. As shown in Figure 3, the measured *HERO* PSF falls off rapidly: 2 orders of magnitude within  $\sim 30$  arcseconds. The dynamic range for well separated sources ( $>50$  arcseconds) is expected to be  $\sim 1000$ .

## 5. DETECTORS

The *FOXSI* program requires a focal plane detector with good energy and spatial resolution, low background, and low power consumption. To meet these requirements, *FOXSI* uses thin double-sided silicon strip detectors (DSSDs) with a fine pitch and low-power front-end ASIC. These detectors were originally developed for the Hard X-ray Imager onboard the Astro-H (formerly NeXT) mission.<sup>7</sup>

The DSSDs are fabricated by orthogonally-implanting n- and p-wells on either side of a monolithic silicon wafer, resulting in sets of segmented strips. An energy deposition event creates electron hole pairs which drift to opposite sides of the silicon. Due to the orthogonality of the strips, detection of the electron and holes give the 2 dimensional position of the event. The *FOXSI* detectors have a pitch of  $75 \mu\text{m}$  corresponding to a spatial resolution of  $\sim 8$  arcseconds at a focal length of 2 m, matching the optical resolution of single shell (7 arcseconds). With a total of 128 strips on each side, the total active area is  $9.6 \times 9.6 \text{ mm}^2$ . The total sensor size is  $11.7 \times 11.7 \text{ mm}^2$ . The detector thickness is  $500 \mu\text{m}$ , providing good efficiency up to  $\sim 15 \text{ keV}$ .

The DSSDs are read out using front-end ASICs developed as a joint effort by ISAS/JAXA and GM-IDEAS. For each DSSD, four ASICs read out a total of 256 strips (128 strips on each side). When an energy deposition event occurs, a fast shaper ( $0.6 \mu\text{s}$  shaping time) and discriminator produce an analog trigger. A slow shaper ( $3 \mu\text{s}$  shaping time) with sample-and-hold circuitry then measures the deposited energy. In this way, data is collected on a per-photon basis. After each trigger, the entire detector is read out.

The ASICs perform AD conversion using Wilkinson-style ramp ADCs and produce a binary map showing which strips have triggered, along with 10-bit data for each channel, a common-mode noise channel, and a diagnostic channel. All channels are converted simultaneously and a serial data stream is clocked out of the ASIC. The entire acquisition takes a maximum of  $185 \mu\text{s}$ . A dedicated FPGA (Actel ProASIC3) clocks the four ASICs, performs data reduction, and sends the data to a formatter for packaging into the final telemetry stream. To meet telemetry constraints ( $300 \text{ counts s}^{-1} \text{ det}^{-1}$ ), the FPGAs perform zero suppression and pedestal subtraction. The highest-value channel data is retained, along with the three adjacent channels and the triggered channel map. Since the ASIC was designed to minimize power consumption each channel requires only  $1 \text{ mW channel}^{-1}$ , for a total of  $0.26 \text{ W detector}^{-1}$ . Spectral tests were performed on a single detector channel (without the ASIC) at  $-20$  degrees Celsius and a bias voltage of  $350 \text{ V}$ , resulting in an energy resolution of  $1.6 \text{ keV}$  (FWHM). The energy resolution for the integrated detector-ASIC system, which will be tested in the fall of 2009, is expected to be  $<1.5 \text{ keV}$ .

A problem unique to strip detectors is “ghosting”. If photons are simultaneously detected at two locations in the detector, four channels will trigger. From these four channels, four possible locations can be reconstructed but only two locations are valid. To mitigate this effect, each *FOXSI* detector is set at a different clocking angle. In this way, the ghost sources will always appear in different locations in different detectors while the true locations stays the same.

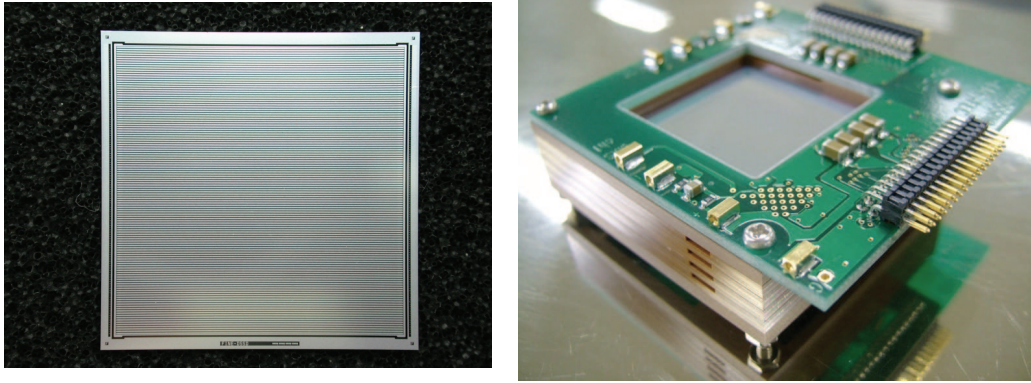


Figure 4. *Left:* A photograph of a preliminary 300  $\mu\text{m}$  thick, 128 strip silicon detector with 150  $\mu\text{m}$  pitch. The *FOXSI* detectors have a pitch of 75  $\mu\text{m}$  and the same number of pixels. The *FOXSI* detector dimensions are 9.6 $\times$ 9.6 mm<sup>2</sup> and will be 500  $\mu\text{m}$  thick. *Right:* A photograph of an integrated detector system similar to the future *FOXSI* system with readout ASICs.

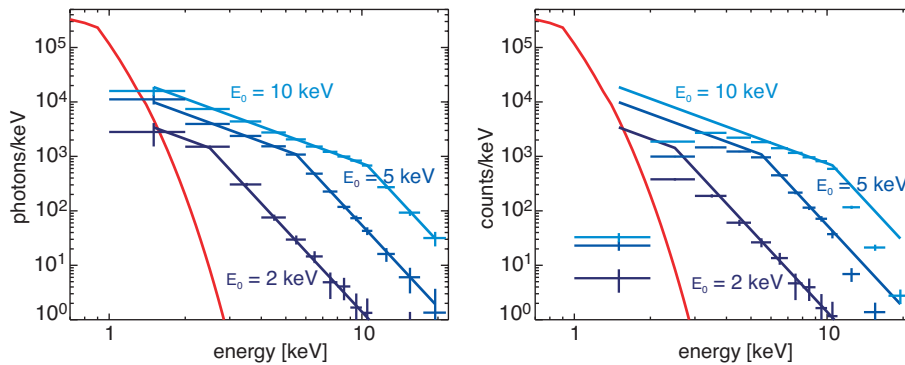


Figure 5. *Left:* Expected X-ray photon spectrum of a quiet Sun nanoflare assuming the heating seen in SXR ( $T=2$  MK,  $EM=10^{44}$  cm<sup>-3</sup>,  $E_{\text{thermal}} = 5 \times 10^{25}$  ergs, duration of 60 s) is produced by nonthermal electrons. Three spectra for different turn-over energies are shown. The photon spectrum is assumed to be a power law with a slope of -5 above the turnover energy,  $E_0$ , and a slope of -1.7 below. The blue lines show the nonthermal spectra with perfect statistics and resolution; the blue data points with error bars are the expected *FOXSI* measurements. The red curve shows the thermal spectra ( $T=2$  MK). *Right:* The count spectrum. At low energies, photons are absorbed by a beryllium entrance window while at high energies the effective area of the telescope is reduced. The expected count rate for the three spectra shown are 14, 91, 245 counts per second, respectively.

## 6. OBSERVATIONS/SCIENCE

The main science goal of *FOXSI* is to explore HXR emissions from the non-flaring Sun\* (for other science targets see Figure 6). The huge increase in sensitivity (a factor of 50) as compared to previous HXR imaging observations provides, for the first time, the opportunity to search for nonthermal HXR emission from supra-thermal electrons (with energies greater than a few keV) and hot thermal plasmas (with temperatures above 8 MK) in the non-flaring corona. These emissions are expected to be present in the nanoflare heating scenario in which a large number of small flares provides the energy input to heat the solar corona. The detection of HXR emission from the non-flaring Sun would provide strong evidence for nanoflare heating, while the absence would call into question nanoflares as a solution to the coronal heating problem.

HXR emission from the non-flaring Sun is expected to be easiest to detect in the  $\sim 5$  to 15 keV range.<sup>10</sup> The *FOXSI* payload was therefore designed to have maximal effective area around 10 keV without consideration of the high energy response. Restricting the energy range of *FOXSI* to energies below 15 keV further simplifies the

\*The difficulty of predicting solar flares together with the restriction of the launch window and the short observation time provided by sounding rockets excludes solar flares as a main science goal.

instrument design as no multi-layer coatings of the grazing incidence optics are needed and Si detectors cover the energy range adequately.

Observations at around 10 keV require a minimum altitude of  $\sim 120$  km to avoid strong atmospheric absorption giving a total observation time (360 s). Thermal events seen in EUV in the quiet Sun indicate heating on time scales of minutes.<sup>5</sup> From EUV observations,<sup>11–13</sup> we estimate  $\sim 10$  to  $\sim 1000$  such events within the *FOXSI* field of view (960 by 960 arcseconds<sup>2</sup>) during the flight. The spatial resolution and dynamic range of *FOXSI* will allow us to separate different events (without resolving individual events). If these quiet-Sun events are similar to regular active-region solar flares, *FOXSI* should clearly detect nonthermal bremsstrahlung emission from the supra-thermal electrons (see Figure 5). The absence of HXR emission would indicate that the thermal EUV events in the quiet Sun are different from regular flare seen in active regions.

As the *FOXSI* field-of-view is smaller than the solar disk, target selection is important. The FOV should include quiet sun and polar areas, avoiding active regions. For the case that no HXR emission is detected from the primary target, a secondary target with higher activity (small active region or X-ray bright point) will be observed during the last two minutes of the flight. This will ensure that the HXR optics will be fully tested for solar observations. In the case that the count rates from the primary target are too high for the *FOXSI* data rate (above 300 counts s<sup>-1</sup> det<sup>-1</sup>), mechanical attenuators can be put in front of the detectors to reduce the low energy photon flux.

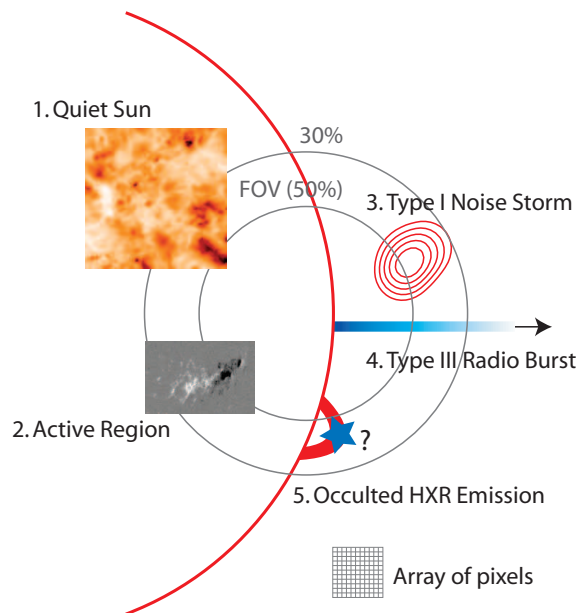


Figure 6. An illustration of all possible *FOXSI* science targets compared to the field-of-view. The field of view is defined as the half power diameter (grey circles). The 30% level contour is also plotted. A sample pixel array (10 by 10 in this case) can be seen in the lower right hand corner though the actual detector will have 128 by 128 pixels covering the entire illustration. The main goal for *FOXSI* is to observe nonthermal electrons through their HXR emission. The primary science targets are the quiet Sun (1) and active-region microflares (2). Other targets associated with nonthermal electron emission, in order of importance, are type I noise storms (3), type III radio bursts (4), and flare loop-top emission (5).

## 7. OUTLOOK AND CONCLUSIONS

HXR grazing-incidence focusing optics are expected to provide the sensitivity and dynamic range needed to image typical solar electron beams as they travel through the corona and image their acceleration region. Furthermore, it should be possible to image the location of energetic electrons producing the large variety of meter and decimeter radio emission<sup>14</sup> (e.g. energetic electrons accelerated at coronal shocks as seen in radio type II bursts). *FOXSI* is expected to be a pathfinder for a future space-based satellite mission. Such a mission is expected to be able to image where electrons are accelerated, along which field lines they travel away from the acceleration site,



where they are stopped, and how some electrons escape into interplanetary space. Additionally, spectroscopy will simultaneously provide quantitative measurements such as the energy spectrum, density, and energy content of the accelerated electrons. Such observations will revolutionize our understanding of particle acceleration in astrophysical plasmas.

The *FOXSI* payload will be recovered and a second scientific flight will likely be proposed. For longer duration observations that will allow us to observe solar flares at higher energies, balloon and satellite versions of *FOXSI* are currently under study. As the HXR emission from solar flares are generally dominated by thermal emission below 20 keV (in some cases up to 30 keV), CdTe detectors (strips or pixels) are needed to extend the energy range into the region where nonthermal bremsstrahlung is observed. Such a system may also make astrophysical observations.

## ACKNOWLEDGMENTS

This effort is funded by under NASA grant NNH06ZDA001N.

## REFERENCES

- [1] Lin, R. P., Dennis, B. R., Hurford, G. J., Smith, D. M., Zehnder, A., Harvey, P. R., Curtis, D. W., Pankow, D., Turin, P., Bester, M., Csillaghy, A., Lewis, M., Madden, N., van Beek, H. F., Appleby, M., Raudorf, T., McTiernan, J., Ramaty, R., Schmahl, E., Schwartz, R., Krucker, S., Abiad, R., Quinn, T., Berg, P., Hashii, M., Sterling, R., Jackson, R., Pratt, R., Campbell, R. D., Malone, D., Landis, D., Barrington-Leigh, C. P., Slassi-Sennou, S., Cork, C., Clark, D., Amato, D., Orwig, L., Boyle, R., Banks, I. S., Shirey, K., Tolbert, A. K., Zarro, D., Snow, F., Thomsen, K., Henneck, R., McHedlishvili, A., Ming, P., Fivian, M., Jordan, J., Wanner, R., Crubb, J., Preble, J., Matranga, M., Benz, A., Hudson, H., Canfield, R. C., Holman, G. D., Crannell, C., Kosugi, T., Emslie, A. G., Vilmer, N., Brown, J. C., Johns-Krull, C., Aschwanden, M., Metcalf, T., and Conway, A., “The Reuven Ramaty High-Energy Solar Spectroscopic Imager (RHESSI),” *Sol. Phys.* **210**, 3–32 (Nov. 2002).
- [2] Hurford, G. J., Schmahl, E. J., Schwartz, R. A., Conway, A. J., Aschwanden, M. J., Csillaghy, A., Dennis, B. R., Johns-Krull, C., Krucker, S., Lin, R. P., McTiernan, J., Metcalf, T. R., Sato, J., and Smith, D. M., “The RHESSI Imaging Concept,” *Sol. Phys.* **210**, 61–86 (Nov. 2002).
- [3] Ramsey, B. D., Alexander, C. D., Apple, J. A., Benson, C. M., Dietz, K. L., Elsner, R. F., Engelhaupt, D. E., Ghosh, K. K., Kolodziejczak, J. J., O’Dell, S. L., Speegle, C. O., Swartz, D. A., and Weisskopf, M. C., “First Images from HERO, a Hard X-Ray Focusing Telescope,” *ApJ* **568**, 432–435 (Mar. 2002).
- [4] Krucker, S. and Benz, A. O., “Are Heating Events in the Quiet Solar Corona Small Flares? Multiwavelength Observations of Individual Events,” *Sol. Phys.* **191**, 341–358 (Feb. 2000).
- [5] Krucker, S., Benz, A. O., Bastian, T. S., and Acton, L. W., “X-Ray Network Flares of the Quiet Sun,” *ApJ* **488**, 499–+ (Oct. 1997).
- [6] Berghmans, D., Clette, F., and Moses, D., “Quiet Sun EUV transient brightenings and turbulence. A panoramic view by EIT on board SOHO,” *A&A* **336**, 1039–1055 (Aug. 1998).
- [7] Kokubun, M., Nakazawa, K., Watanabe, S., Fukazawa, Y., Kataoka, J., Katagiri, H., Mizuno, T., Makishima, K., Ohno, M., Sato, G., Sato, R., Tajima, H., Takahashi, T., Tamagawa, T., Tanaka, T., Tashiro, M., Takahashi, H., Terada, Y., Uchiyama, Y., Urata, Y., Yamaoka, K., Takeda, S., Kishishita, T., Ushio, M., Katsuta, J., Ishikawa, S., Odaka, H., Aono, H., Sugimoto, S., Koseki, Y., Kitaguchi, T., Enoto, T., Yamada, S., Yuasa, T., Ueda, T., Uehara, Y., Okuyama, S., Yasuda, H., Nishino, S., Umeki, Y., Hayashi, K., Matsuoka, M., Ikejiri, Y., Endo, A., Yaji, Y., Kodaka, N., Iwakiri, W., Kouzu, T., Sugawara, T., Harayama, A., and Nakahira, S., “Hard X-ray imager (HXI) for the NeXT mission,” in [*Society of Photo-Optical Instrumentation Engineers (SPIE) Conference Series*], *Society of Photo-Optical Instrumentation Engineers (SPIE) Conference Series* **7011** (Aug. 2008).
- [8] Cluzet, G., Doenecke, J., Vollmer, K., and Patti, B., “HUYGENS Probe: Thermal Design, Test, Flight Comparison, and Descent Prediction,” *SAE Technical Paper Series 28th International Conference on Environmental Systems, Danvers, Massachusetts* **981644**, (1998).

- [9] Gubarev, M., Arnold, W., Benson, C., Kester, T., Lehner, D., Ramsey, B., and Upton, R., “Mounting and alignment of full-shell replicated x-ray optics,” in [*Society of Photo-Optical Instrumentation Engineers (SPIE) Conference Series*], *Society of Photo-Optical Instrumentation Engineers (SPIE) Conference Series* **6688** (Sept. 2007).
- [10] Hannah, I. G., Hurford, G. J., Hudson, H. S., Lin, R. P., and van Bibber, K., “First Limits on the 3-200 keV X-Ray Spectrum of the Quiet Sun Using RHESSI,” *ApJ* **659**, L77–L80 (Apr. 2007).
- [11] Krucker, S. and Benz, A. O., “Energy Distribution of Heating Processes in the Quiet Solar Corona,” *ApJ* **501**, L213+ (July 1998).
- [12] Aschwanden, M. J., Nightingale, R. W., Tarbell, T. D., and Wolfson, C. J., “Time Variability of the “Quiet” Sun Observed with TRACE. I. Instrumental Effects, Event Detection, and Discrimination of Extreme-Ultraviolet Microflares,” *ApJ* **535**, 1027–1046 (June 2000).
- [13] Parnell, C. E. and Jupp, P. E., “Statistical Analysis of the Energy Distribution of Nanoflares in the Quiet Sun,” *ApJ* **529**, 554–569 (Jan. 2000).
- [14] Pick, M. and Vilmer, N., “Sixty-five years of solar radioastronomy: flares, coronal mass ejections and Sun Earth connection,” *A&A Rev.* **16**, 1–153 (Oct. 2008).